Challenge Journal of Structural Mechanics

Research Article

Experimental study on the rotation capacity of bolted and welded beam-to-column connection using cold-formed steel sections

Mahyar Maali [a,*], Merve Sağıroğlu [a], Mahmut Kılıç [b], Abdulkadir Cüneyt Aydın [b]

[a] *Department of Civil Engineering, Erzurum Technical University, 25050 Erzurum, Türkiye*
[b] *Department of Civil Engineering, Atatürk University, 25240 Erzurum, Türkiye*

ABSTRACT

This paper investigates new bolted and welded beam-to-column connection types on the cold-formed steel sections (CFS) and their behaviors determined using full-scale experiments. This study aimed to analyze the influence of weld/bolt connections based on CFS profile and failure modes to provide the necessary data for improving Eurocode 3. In contrast, the rotation and ductility of a joint of the welded connection are lower than the bolted connection. Thus, the bolted connection exhibits a semi-rigid behavior–also, the energy dissipation capacity values in the bolted connection are bigger than welded connection. Thus, the bolded connection has a semi-rigid behavior. Also, model failure is determined by the type of connection (bolted and welded). The rotation and ductility of a joint of the welded connection are lower than the bolted connection. Thus, the bolted connection exhibits a semi-rigid behavior–also, the energy dissipation capacity values in the bolted connection are bigger than welded connection. Furthermore, the specimens of the welded connection have rigid behavior in the failure modes.

ARTICLE INFO

Article history:
Received 21 April 2022
Revised 13 May 2022
Accepted 9 June 2022

Keywords:
Experimental study
Moment–rotation curves
CFS profile
Weld/bolt connection
Eurocode 3

1. Introduction

The use of light steel in a structural system has been increasing rapidly in recent years because of many advantages such as being economical, faster construction, and lightness. However, the existing design guides concerning domestic and foreign standards are not as straightforward as those of conventional steel structures. The most important area in steel column beam elements is the connection area. In addition, connecting tools are made in light steel (cold-formed steel) with various methods (bolt, weld, and screw). It is necessary to consider the behavior of connections in the design and analysis of steel frames because it represents the actual behavior (Sagiroglu and Aydin 2015). Beam-column connections are considered rigid or pinned in traditional steel structures calculation methods. Although this idealization of the joint behavior simplifies the analysis process, it results in differences between the idealized behavior and the actual behavior of the structure. According to these theoretical idealizations;

- In rigid connections, there is no local rotation in the elements; when an external moment acts, this moment is distributed in proportion to the stiffness of the elements.
- Again, according to this assumption, local rotation occurs in an articulated joint. However, the elements do not transfer moment.

However, the joints are neither perfectly rigid nor fully articulated in reality. Joints used in steel frames exhibit semi-rigid and non-linear behavior. In recent studies, it has been proven that accepting the joint as semi-rigid gives more accurate results. In addition, some studies have shown that semi-rigid joint performance provides benefits such as reduction in joint elements, size, and weight (Bagheri et al. 2012). Fig. 1 shows the behavior of the steel beam to column connection.

Recently, many experimental studies have been carried out to examine the actual behavior of cold-formed steel beam-column connections. However, after 1950, experimental studies focused on semi-rigid connections. Therefore, cold-formed steel beam-to-column connec-

* *Corresponding author*. Tel.: 444-5-388 ; Fax: +90-442-230-0036 ; E-mail address: mahyar.maali@erzurum.edu.tr (M. Maali)
ISSN: 2149-8024 / DOI: https://doi.org/10.20528/cjsmec.2022.04.001

tions types investigated in recent years have increased, and many researchers are trying to obtain the actual behavior of the connection. In addition, experimental research on this topic is limited due to the high cost of experimenting. Therefore, both numerical and experimental studies in the literature are examined, and it is seen that the effort to obtain the actual behavior on these issues is limited. Table 1 summarizes the cold-formed steel beam-to-column connections experiments performed in the last ten years.

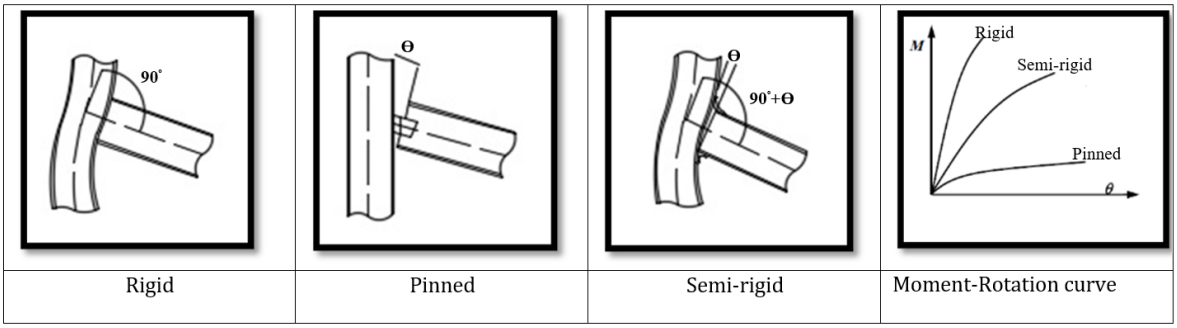

Rigid	Pinned	Semi-rigid	Moment-Rotation curve

Fig. 1. Joint types.

Table 1. Cold-formed beam-to column connection experiments.

Author	Aim of research (CFS)	Number of experiments
Bagheri et al. (2012)	Moment resistance determined by the earthquake	3
Anwer et al. (2012)	Bolted connections for the channel sections	10
Torabian et al. (2015)	Lipped channel	20
Freya et al. (2016)	Semi rigid connections	2
Serror et al. (2016)	Rotation capacity	10
Maali et al. (2018a9	Screwed beam-to-column connections	3
Zhao et al. (2018)	Hysteretic behaviour of steel storage rack beam-to-upright boltless connections	8
Bucmys et al. (2018)	Bolted gusset plate joints	3
Ayhan and Schafer (2019)	Floor-to-wall connection	27
Benchaphong et al. (2021)	Bolted connection in the trusses	9

In this research, the beam-to-column connection of endplate and double C profile beam jointed with gusset plate and bolted and welded was selected. The moment rotation (M-θ) behavior, moment-rotation characteristic values, and failure modes of the bolted and welded beam-to-column connections in the cold-formed steel structures with various dimensions of elements have been evaluated and compared. Various beam thicknesses and gusset plate thicknesses have been used to make a meaningful comparison. Also, the welded group was compared to bolted group specimens tests. Six cold-formed steel connections in two groups (welded and bolted) have been tested based on these parameters. Finally, this paper presents the evolutionary development to use bolted-welded connections by beginning by using different beams and different gusset plate thicknesses.

2. Specimens Test Details

This paper presents the six experimental tests in two groups that studied the rotation capacity of bolted and welded beam-column connections using cold-formed steel sections under statically loaded. All experiments were done on a 1/1 scale. The experimental program is shown in Fig. 2 and detailed in Table 2. First, the gusset plate with various thicknesses was welded (the manual metal arc welding process) to the end plate with a thickness equal to 10 mm using a continuous 45° fillet weld with the down-hand position for the workshop (Aydın et al. 2015a, 2015b; Maali et al. 2015). Second, the stiffener with 2mm thicknesses was welded to the C Profile. The gusset plate CFS profile, plate stiffener, and end-plate properties were S235. The weld length was 50mm with 2mm weld thickness in the weld group specimens test. The bolt's diameter was M8 with grade 8.8. The beam is made of back-to-back light steel channel sections composed of 13 bolts, and the beam-to-column connection was a connection area with nine bolts. Thus, this study aimed to analyse the influence of various beam thicknesses and used stiffener in the CFS beams, with gusset plate with various thicknesses on the behavior of moment-rotation curve, to provide the necessary data for improving Eurocode 3 (Eurocode 3 2005) and also, compare the moment-rotation curves results of the experiments in the welded group and the test results in the bolted group.

The gusset plate thickness is indicated in Table 2 by the letters "P", the beam thickness is labelled as "C", the bolted connection is labelled as "B", the welded connection is labelled as "W", while the use of stiffener is labelled as "S".

Table 2. Properties of the test specimens.

Group	Test Specimen	Gusset plate thickness (P, mm)	Use of stiffeners	Bolted diameter (mm)	Beam thickness (C, mm)	Beam Stiffeners thickness (mm)	Length of beam and column (mm)	Column Profile (S235)
Bolted	B-C1-P1-S	1.0	YES	8.8	1.0	2.0	1500	HE280B
	B-C1.5-P1.5-S	1.5	YES	8.8	1.5	2.0		
	B-C2-P2-S	2.0	YES	8.8	2.0	2.0		
Weld	W-C1-P1-S	1.0	YES	-	1.0	2.0	1500	HE280B
	W-C1.5-P1.5-S	1.5	YES	-	1.5	2.0		
	W-C2-P2-S	2.0	YES	-	2.0	2.0		

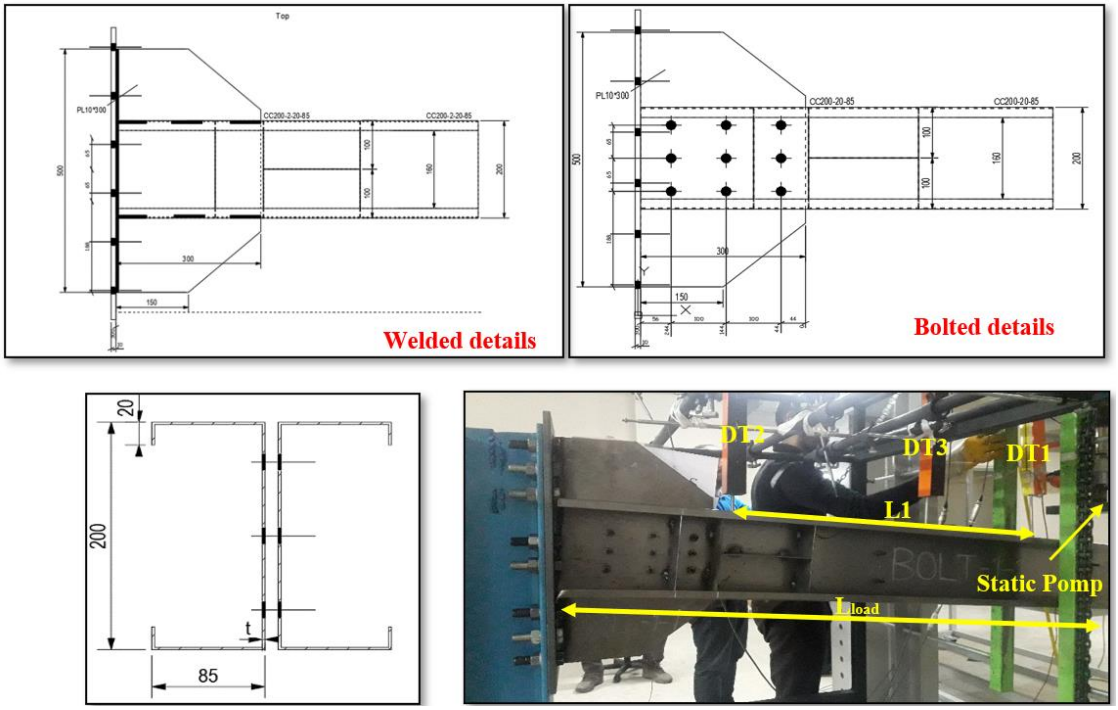

Fig. 2. The beam-to-column connection details (CFS beams details: C200-20-85).

The hydraulic pump (250kN with 300mm stroke) measured applied load (P) by a load cell; displacement of the beam measured by three LVDTs (300 mm) (LVDTs, shown as DT in Fig. 2). The bending moment obtained by (Aydın et. al. 2015; Maali 2018; Maali et. al. 2018b, 2019; Kılıç et al. 2019) research:

$$M = P \cdot L_{\text{load}} \tag{1}$$

$$\theta = \frac{\arctan\left[\delta_{DT1} - \delta_{DT2} - \left(\left(-\frac{P}{EI}\right)\left(\frac{X_{DT1}^3}{6} - \frac{L_{\text{load}} X_{DT2}^2}{2}\right)\right)\right]}{L1} \tag{2}$$

where I is the moment of inertia and E is the Young's modulus of beam. The rotational deformation of the joint (θ) is equal to the connection rotation. δ_{DT-1}, δ_{DT-2}, x_{DT-1}^3 and x_{DT-2}^2 represent the location and distance between LVDTs.

3. Moment-Rotation Curve

The M–θ curve for connection obtained of the Eurocode 3 Part 1.8 BS EN (1993) is given in Fig 3.

Also, the ductility of a joint (Ψ_j) and the rotation values at the maximum load and corresponding ductility levels ($\Psi_{j.\text{maxload}}$) given by Maali et al. (2018b):

$$\Psi_j = \frac{\theta_{Cd}}{\theta_{M.Rd}} \tag{3}$$

$$\Psi_{j.\text{maxload}} = \frac{\theta_{M.j.\max}}{\theta_{M.Rd}} \tag{4}$$

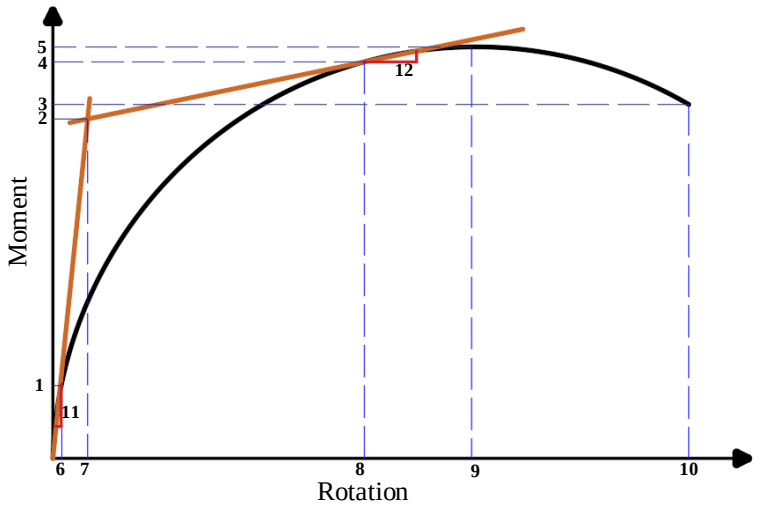

1. Lower moment in the elastic area, M_{mink-R}
2. The plastic flexural resistance, $M_{j.Rd}$
3. The bending moment capacity, $M_{\theta.Cd}$
4. Upper moment in the plastic area, M_{supk-R}
5. The maximum bending moment, $M_{j.max}$
6. The rotation lower moment in the elastic area, θ_{mink-R}
7. The rotation plastic flexural resistance, $\theta_{M.Rd}$
8. The rotation upper moment in the plastic area, θ_{supk-R}
9. The rotation maximum bending moment, $\theta_{M.j.max}$
10. The rotation capacity, θ_{cd}
11. The initial stiffness, $S_{j.ini}$
12. Post-limit stiffness, $S_{j.p-l}$

Fig. 3. Moment–rotation curve characteristics of the Eurocode 3.

4. Test Results

In this study, the moment-rotation curves of six cold-formed steel beam-to-column under static load are drawn, and characteristic features such as moment resistance, stiffness, rotation capacity, the ductility of a joint, and energy dissipation are represented by moment-rotation curves are determined. Fig. 4 and Table 3 show the moment–rotation characteristics of the two groups.

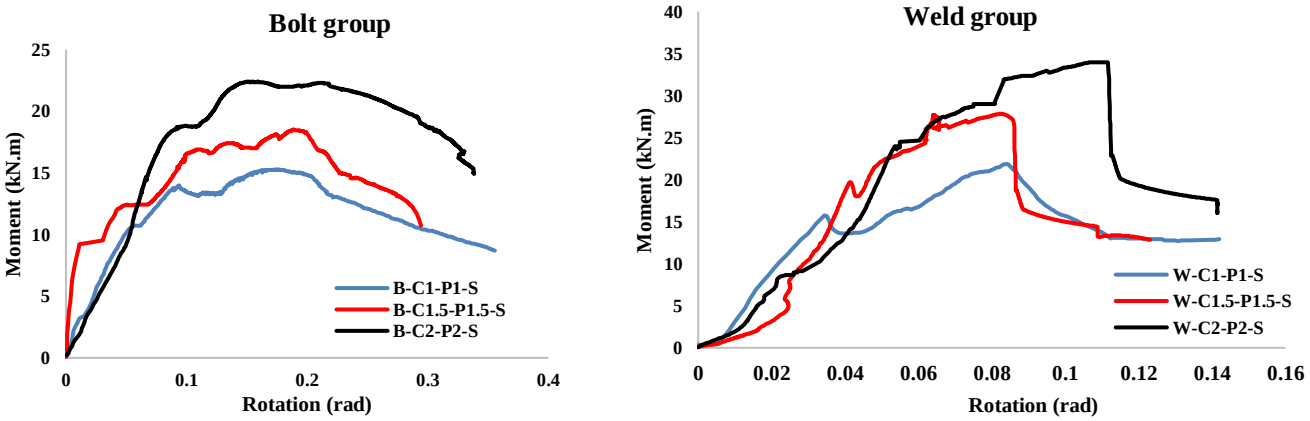

Fig. 4. Moment-rotation curve of the two group.

Table 3. Moment-rotation characteristic properties for all specimens' tests.

Group	Experiment	Resistance (kN.m)			Stiffness (kN m/rad)			Rotation (rad)			Ductility of a joint		Energy dissipation (kN.m.rad)
		$M_{j.Rd}$	$M_{j.max}$	$M_{j.max}/M_{j.R}$	$S_{j.ini}$	$S_{j.p-1}$	$S_{j.ini}/S_{j.p-}$	θ_{MJRd}	$\theta_{Mj.max}$	θ_{Cd}	$\Psi_j=\frac{\theta Cd}{\theta MJRd}$	$\Psi_{j.maxload}=\frac{\theta Mj.max}{\theta MJRd}$	E
Bolt	B-C1-P1-S	13.42	15.28	1.14	0.38	3.87	0.098	0.065	0.17	0.35	5.39	2.62	3.41
	B-C1.5-P1.5-S	14.22	18.39	1.29	0.14	4.16	0.033	0.031	0.191	0.29	9.35	6.16	3.89
	B-C2-P2-S	21.03	22.37	1.06	0.59	7.36	0.08	0.103	0.15	0.34	3.30	1.46	4.14
Weld	W-C1-P1-S	16.80	21.83	1.30	0.58	2.91	0.199	0.036	0.08	0.141	3.91	2.22	0.98
	W-C1.5-P1.5-S	22.78	27.61	1.21	0.46	2.56	0.18	0.044	0.08	0.123	2.80	1.82	1.82
	W-C2-P2-S	29.07	32.71	1.12	1.1	7.72	0.142	0.071	0.11	0.14	1.97	1.55	2.57

4.1. Bolt group

Fig. 4 and Table 3 show that the plastic flexural resistance and the maximum bending moment values increased by about 5.6%–36.18% and 16.91%–31.69%, respectively, with increased gusset plate thicknesses and beam thicknesses of the 1mm to 2mm. Also, the ideal value for the $M_{j.\max}/M_{j.Rd}$ is between 1 and 1.3. Table 3 shows that the $M_{j.\max}/M_{j.Rd}$ for the B-C1.5-P1.5-S and B-C1-P1-S specimens test increased by about 11.62%, increasing beam thicknesses and gusset thickness of 1 to 1.5mm. While, the $M_{j.\max}/M_{j.Rd}$ for the between B-C2-P2-S and B-C1-P1-S and between B-C2-P2-S and B-C1.5-P1.5-S specimens test decreased by about 7.55% and 21.70%, respectively, with an increase in beam thicknesses and gusset thicknesses. Table 3 shows that the $S_{j.ini}/S_{j.p^{-1}}$values decreased by about 22.5%–196.97%, respectively, with increased gusset plate thicknesses and beam thicknesses of 1mm to 2mm. Additionally, Table 3 shows that the θ_{MjRd} value for B-C1.5-P1.5-S and B-C1-P1-S specimens test decreased by about 109.67%, increasing beam thicknesses and gusset thicknesses of the 1 to 1.5mm. While the θ_{MjRd} value for the between B-C2-P2-S and B-C1-P1-S and between B-C2-P2-S and B-C1.5-P1.5-S specimens test increased by about 36.89% and 69.90%, respectively, with an increase in beam thicknesses and gusset thicknesses. Moreover, Table 3 shows that $\theta_{Mj.max}$ value for the B-C1.5-P1.5-S and B-C1-P1-S specimens test increased by about 10.99%, increasing beam thicknesses and gusset thicknesses of the 1 to 1.5mm. While the $\theta_{Mj.max}$ value for the between B-C2-P2-S and B-C1-P1-S and between B-C2-P2-S and B-C1.5-P1.5-S specimens test decreased by about 13.33% and 27.33%, respectively, with an increase in beam and gusset thicknesses. In addition, Table 3 shows that θ_{Cd} value for the B-C2-P2-S, B-C1.5-P1.5-S, and B-C1-P1-S specimens test decreased by about 20.68%-2.94% with an increase in beam thicknesses and gusset thicknesses of the 1 to 2mm. Also, Table 3 shows that the Ψj for the B-C1.5-P1.5-S and B-C1-P1-S specimens test increased by about 42.35%, with an increase in beam thicknesses and gusset thicknesses of the 1 to 1.5mm. While, the Ψ_j for the between B-C2-P2-S and B-C1-P1-S and between B-C2-P2-S and B-C1.5-P1.5-S specimens test decreased by about 63.33% 183.33%, respectively, with an increase in beam thicknesses and gusset thicknesses. Moreover, Table 3 shows that the $\Psi_{j.\text{maxload}}$ for the B-C1.5-P1.5-S and B-C1-P1-S specimens test increased by about 57.46%, with an increase in beam thicknesses and gusset thicknesses of the 1 to 1.5mm. While, the $\Psi_{j.\text{maxload}}$ for the between B-C2-P2-S and B-C1-P1-S and between B-C2-P2-S and B-C1.5-P1.5-S specimens test decreased by about 79.45% and 321.92%, respectively, with an increase in beam thicknesses and gusset thicknesses. Also, the energy dissipation capacity increased by about 12.33%-17.63% with an increase in beam thicknesses and gusset thicknesses of 1 to 2mm. Generally, the moment resistance, critical rotation capacity, and energy dissipation capacity increased with an increase in beam thicknesses and gusset thicknesses of 1 to 2mm. While the stiffness decreased with an increase in beam thicknesses and gusset thicknesses of 1 to 2mm.

4.2. Weld group

Fig. 4 and Table 3 show that the plastic flexural resistance and the maximum bending moment values increased by about 26.25%–42.21% and 20.93%–33.26%, respectively, with increased gusset plate thicknesses and beam thicknesses of the 1mm to 2mm. Also, the $S_{j.ini}/S_{j.p^{-1}}$ values decreased by about 10.55%–40.14%, respectively, with increased gusset plate thicknesses and beam thicknesses of 1mm to 2mm. Also, the θ_{MjRd} value increased by about 18.18%-49.29%, increasing beam thicknesses and gusset thicknesses of 1 to 2mm. Moreover, the $\theta_{Mj.max}$ value increased by about 27.27% with an increase in beam thicknesses and gusset thicknesses 1 to 2mm. While the θ_{Cd} value decreased by about 0.71%-14.63% with an increase in beam thicknesses and gusset thicknesses of 1 to 2mm. In addition, Table 3 shows that the Ψ_j and $\Psi_{j.\text{maxload}}$ values decreased by about 39.64%-194% and 21.97%-43.22%, receptively, with an increase in beam thicknesses and gusset thicknesses of the 1 to 2mm. Also, the energy dissipation capacity increased by about 19.71%-30.08% with an increase in beam thicknesses and gusset thicknesses of 1 to 2mm. Generally, the moment resistance, plastic flexural rotation capacity, and maximum rotation capacity increased with beam thicknesses and gusset thicknesses of 1 to 2mm. While the stiffness, critical rotation capacity, energy dissipation capacity, and the ductility of a joint decreased with an increase in beam thicknesses and gusset thicknesses of 1 to 2mm.

4.3. Comparison between bolt and weld group

Fig. 5 and Table 4 show the comparison between bolt and weld groups. Fig. 5 and Table 4 show the following:

- The $M_{j.Rd}$, $M_{j.\max}$ and $S_{j.ini}/S_{j.p^{-1}}$ values for the W-C1-P1-S and B-C1-P1-S, W-C1.5-P1.5-S and B-C1.5-P1.5-S, W-C2-P2-S and B-C2-P2-S models increased by about 20.12%, 37.57%, 27.66%, 30%, 33.39%, 31.61%, 50.75%, 81.66%, and 43.66%, respectively, with used welded connection compared to bolded connection. Therefore, the welded connection exhibits a rigid behavior.
- The θ_{MjRd}, $\theta(M_{j.\max})$, θ_{Cd}, Ψ_j and $\Psi_{j.\text{maxload}}$ values for the W-C1-P1-S and B-C1-P1-S, W-C1.5-P1.5-S and B-C1.5-P1.5-S, W-C2-P2-S and B-C2-P2-S models decreased by about 80.55%, 45.07%, 112.5%, 138.8%, 36.36%, 148.22%, 135.77%, 142.86%, 37.85%, 233.93%, 67.52%, 18.01%, and 238.46%, respectively, with used welded connection compared to bolded connection. While, The θ_{MjRd}, and $\Psi_{j.\text{maxload}}$ values for the W-C1.5-P1.5-S and B-C1.5-P1.5-S, W-C2-P2-S and B-C2-P2-S models increased by about 29.55%, and 5.81%, respectively, with used welded connection compared to bolded connection. Hence, the rotation and ductility of a joint of the welded connection lower than the bolted connection. Thus. The bolted connection exhibits a semi-rigid behavior.
- The energy dissipation capacity values for the W-C1-P1-S and B-C1-P1-S, W-C1.5-P1.5-S and B-C1.5-P1.5-S, W-C2-P2-S and B-C2-P2-S models decreased by about -247.96%, -113.74% and -61.09%, respect-

tively, with used welded connection compared to bolded connection. Therefore, the energy dissipation capacity values in the bolted connection are bigger than welded connection. Thus, the bolded connection has a semi-rigid behavior.

Generally, the rotation and ductility of a joint of the welded connection are lower than the bolted connection. Thus. The bolted connection exhibits a semi-rigid behaviour also, the energy dissipation capacity values in the bolted connection are bigger than welded connection. Thus, the bolded connection has a semi-rigid behavior.

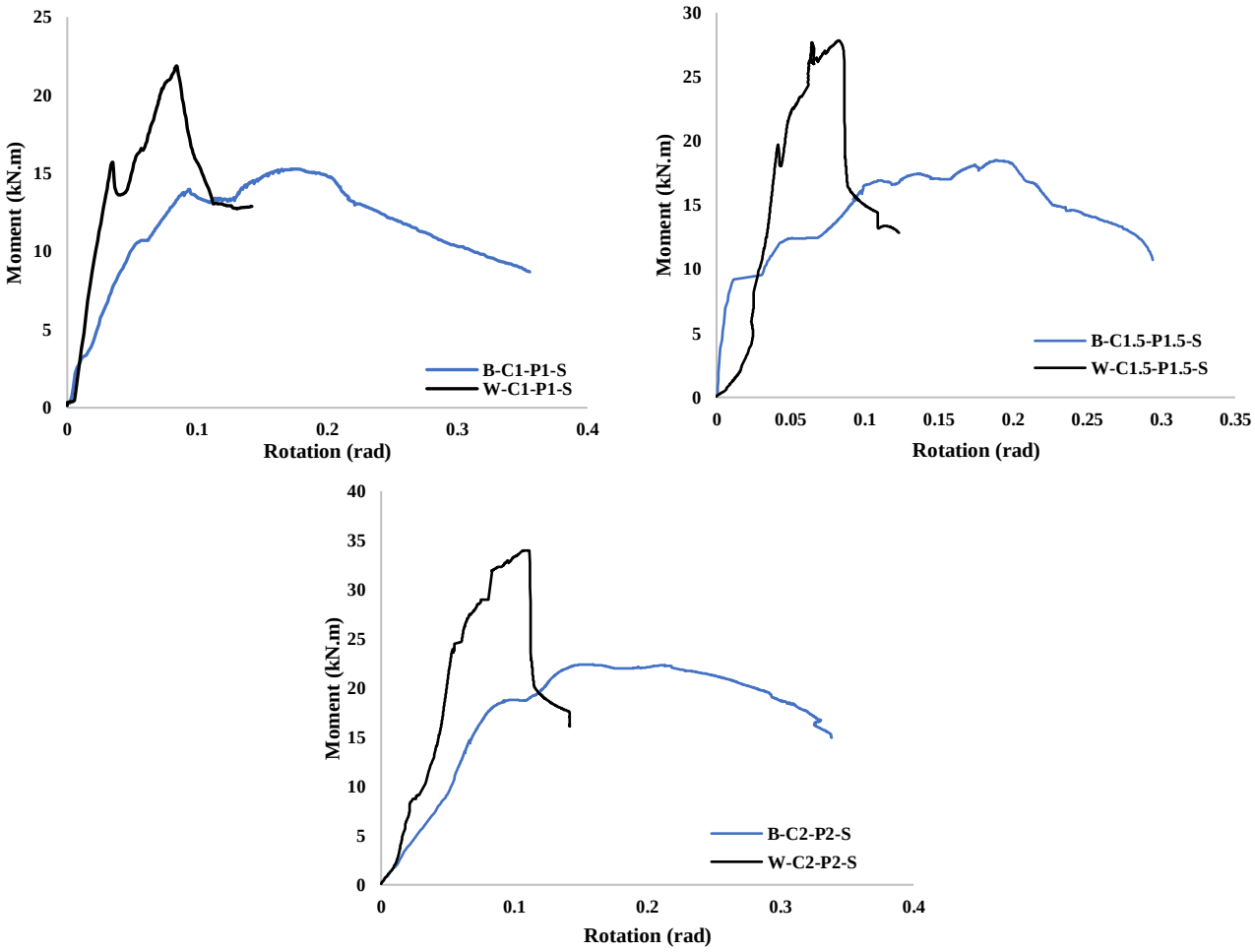

Fig. 5. The moment-rotation characteristics comparison between test specimens.

Table 4. The moment-rotation characteristics comparison for all test specimens.

Experiment	$M_{j.Rd}$	$M_{j.\max}$	$S_{j.ini}/S_{j.p^{-1}}$	θ_{MjRd}	$\theta_{Mj.max}$	θ_{Cd}	Ψ_j	$\Psi_{j.\text{maxload}}$	Energy Dissipation
Percent W-C1-P1-S to B-C1-P1-S (%)	20.12	30.00	50.75	-80.55	-112.50	-148.22	-37.85	-18.01	-247.96
Percent W-C1.5-P1.5-S to B-C1.5-P1.5-S (%)	37.57	33.39	81.66	29.55	-138.80	-135.77	-233.93	-238.46	-113.74
Percent W-C2-P2-S to B-C2-P2-S (%)	27.66	31.61	43.66	-45.07	-36.36	-142.86	-67.52	5.81	-61.09

4.4. Failure modes

Fig. 6 shows the test specimens' collapse modes. There are three types of failure modes for bolted connections in Eurocode 3 (1993); there are three types of failure modes the first is only plate yielding, the second is plate yielding with bolt breakage, and the third is only bolt breakage. Therefore, comparisons of failure modes were made as follows, according to Fig. 6: in the bolt's connection specimens test, all specimens' tests. The collapse occurred with the yield gusset plate with tear gusset. Also, all models were without the bolts failing, and the shape of the gusset plate after it collapsed was similar to the sinus shape. Thus, failure modes in the bolted connection occurred in the second mode in Eurocode 3 (1993). In the welded connection specimens test, in the all-specimens tests, the col-

lapse occurred with the yield gusset plate with the sharing welding in the end-plate area. Also, all model collapse occurred with the buckled C profile beam. Generally, model failure is determined by the type of connection (bolted and welded). Furthermore, the specimens of the welded connection have rigid behavior in the failure modes.

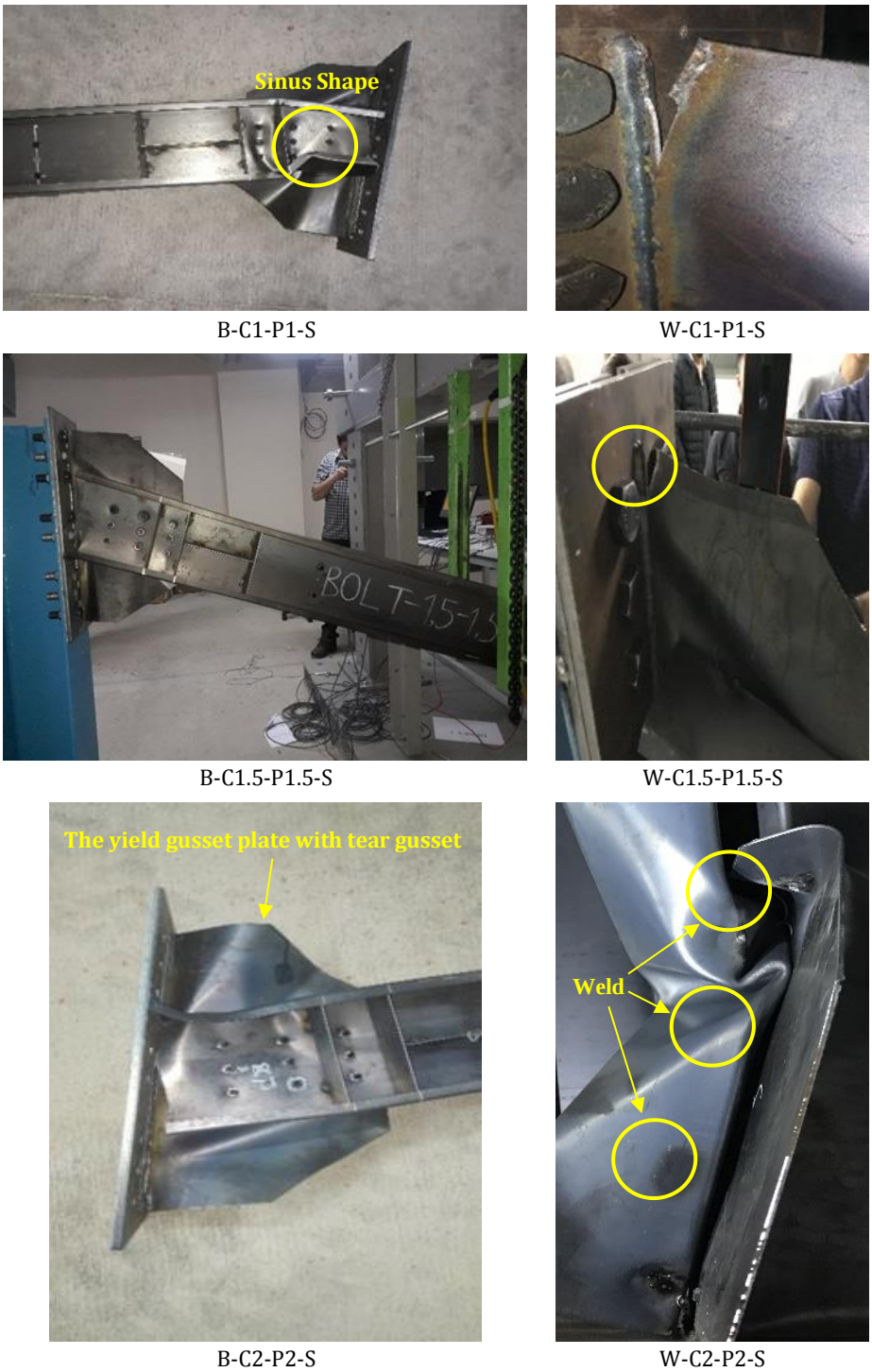

Fig. 6. Collapse modes of test specimens and comparing collapse mode.

5. Conclusions

The aim of this study was studied on the rotation capacity of bolted and welded beam-column connections using cold-formed steel sections. The main conclusions can be summarized as follows:

- Bolted connection: the moment resistance, critical rotation capacity, and energy dissipation capacity increased with beam thicknesses and gusset thicknesses of 1 to 2mm. In contrast, the stiffness decreased with an increase in beam thicknesses and gusset thicknesses of 1 to 2mm.

- Welded connection: the moment resistance, plastic flexural rotation capacity, and maximum rotation capacity increased with beam thicknesses and gusset thicknesses of 1 to 2mm. While the stiffness, critical rotation capacity, energy dissipation capacity, and the ductility of a joint decreased with an increase in beam thicknesses and gusset thicknesses of 1 to 2mm.
- Comparison between bolt and weld group: the rotation and ductility of a joint of the welded connection lower than the bolted connection. Thus, the bolted connection exhibits a semi-rigid behaviour also, the energy dissipation capacity values in the bolted connection are bigger than welded connection. Thus, the bolded connection has a semi-rigid behavior.
- Failure modes: model failure is determined by the type of connection (bolted and welded). Furthermore, the specimens of the welded connection have rigid behavior in the failure modes.

Acknowledgements

None declared.

Funding

The authors received no financial support for the research, authorship, and/or publication of this manuscript.

Conflict of Interest

The authors declared no potential conflicts of interest with respect to the research, authorship, and/or publication of this manuscript.

REFERENCES

Anwer B, Saad S, Osman H (2012). Structural performance of bolted moment connections among single cold-formed channel sections. *International Journal of Engineering and Technology*, 2(4), 599-607.

Aydin AC, Maali M, Kiliç M, Sağıroğlu M (2015a). Experimental investigation of sinus beams with end-plate connections. *Thin-Walled Structure,* 97, 35-43.

Aydin AC, Kiliç M, Maali M, Sağıroğlu M (2015b). Experimental assessment of the semi-rigid connections behavior with angles and stiffeners. *Journal of Constructional Steel Research,* 114, 338-348.

Ayhan D, Schafer BW (2019). Cold-formed steel ledger-framed construction floor-to-wall connection behavior and strength. *Journal of Constructional Steel Research*, 156, 215-226.

Bagheri SA, Petkovski M, Pilakoutas K, Mirghaderi R (2012). Development of cold-formed steel elements for earthquake resistant moment frame buildings. *Thin-Walled Structures*, 53, 99-108.

Benchaphong A, Hongthong R, Benchanukrom S, Konkong N (2021). Stiffness prediction for bolted moment-connections in cold-formed steel trusses. *Engineering Review,* 41(1), 69-84.

BS EN 1993-1-8 (2005). Eurocode 3. Design of Steel Structures Design of Joints.

Bučmys Ž, Daniūnas A, Jaspart JP, Demonceau JF (2018). A component method for cold-formed steel beam-to-column bolted gusset plate joints. *Thin-Walled Structures*, 123, 520-527.

Freya R, Senthil R, Merin WJ, Saravanakumar R, Kuber K, Gowtham M (2016). Behaviour of cold-formed steel semi rigid connections. *Wei-Wen Yu International Specialty Conference on Cold-Formed Steel Structures*, 4.

Kılıç M, Maali M, Aydın AC (2019). The preliminary unıaxıal compressıon behavior of corrugated cold formed steel members. *Architecture Civil Engineering, Environment,* 12(2), 105 - 116

Maali M (2018). Dikey berkitmeli alın levhalı kiriş-kolon birleşimlerin davranışının deneysel olarak incelenmesi. *Gümüşhane University Journal of Science and Technology*, 8(2), 255-263. (in Turkish)

Maali M, Aydin AC, Sağıroğlu M (2015). Investigation of innovative steel runway beam in industrial building. *Sadhana*, 40(7), 2239-2251.

Maali M, Sagiroglu M, Solak MS (2018a). Experimental behavior of screwed beam-to-column connections in cold-formed steel frames. *Arabian Journal of Geosciences,* 11(9), 1-6.

Maali M, Kılıc M, Sagıroglu M, Aydın AC (2018b). Experimental behavior of bolted t-stub connections with IPE standard profile. *Journal of Civil & Environmental Engineering*, 8(3), 1-8.

Maali M, Kılıç M, Aydın AC (2019). Experimental behaviour of bolted connections with stiffeners. *Steel Construction,* 12(2), 105-113.

Sagiroglu M, Aydin AC (2015). Design and analysis of non-linear space frames with semi-rigid connections. *Steel and Composite Structures,* 18(6), 1405-1421.

Serror MH, Hassan EM, Mourad SA (2016). Experimental study on the rotation capacity of cold-formed steel beams. *Journal of Constructional Steel Research,* 121, 216-228.

Torabian S, Zheng B, Schafer BW (2015). Experimental response of cold-formed steel lipped channel beam-columns. *Thin-Walled Structures*, 89, 152-168.

Zhao Z, Dai L, Rasmussen KJR (2018). Hysteretic behaviour of steel storage rack beam-to-upright boltless connections. *Journal of Constructional Steel Research,* 144, 81-105.